NASA TECHNICAL NOTE

NASA TN D-8054

2. u/u

x.

FREE-FLIGHT MODEL INVESTIGATION
OF A VERTICAL-ATTITUDE VTOL FIGHTER

William A. Newsom, Jr., and Ernie L. Anglin

*Langley Research Center
Hampton, Va. 23665*

1. Report No. NASA TN D-8054	2. Government Accession No.	3. Recipient's Catalog No.
4. Title and Subtitle FREE-FLIGHT MODEL INVESTIGATION OF A VERTICAL-ATTITUDE VTOL FIGHTER		5. Report Date September 1975
		6. Performing Organization Code
7. Author(s) William A. Newsom, Jr., and Ernie L. Anglin		8. Performing Organization Report No. L-10345
9. Performing Organization Name and Address NASA Langley Research Center Hampton, Va. 23665		10. Work Unit No. 505-10-31-01
		11. Contract or Grant No.
12. Sponsoring Agency Name and Address National Aeronautics and Space Administration Washington, D.C. 20546		13. Type of Report and Period Covered Technical Note
		14. Sponsoring Agency Code

15. Supplementary Notes

Technical Film Supplement L-1186 available on request.

16. Abstract

The tests were made in the Langley full-scale tunnel and included a study of the stability and control characteristics of delta- and swept-wing configurations from hovering through the transition to normal forward flight. Static force tests were also conducted to aid in the analysis of the flight tests. With conventional artificial rate stabilization, very smooth transitions could be made consistently with relatively little difficulty. Because of the lower apparent damping and a tendency to diverge in yaw, however, the swept-wing configuration was considered to be much more difficult to fly than the delta-wing configuration. With rate dampers off, both configurations were very difficult to control and the control power needed for satisfactory flights was substantially higher than with the rate dampers operating.

17. Key Words (Suggested by Author(s)) VTOL Stability	18. Distribution Statement Unclassified — Unlimited Subject Category 02

19. Security Classif. (of this report) Unclassified	20. Security Classif. (of this page) Unclassified	21. No. of Pages 32	22. Price* $3.75

FREE-FLIGHT MODEL INVESTIGATION OF A
VERTICAL-ATTITUDE VTOL FIGHTER

William A. Newsom, Jr., and Ernie L. Anglin
Langley Research Center

SUMMARY

Free-flight tests were made using a model of a vertical-attitude VTOL fighter with a pivoted forebody (nose-cockpit) design. The tests were conducted in the Langley full-scale tunnel and included a study of delta- and swept-wing configurations from hovering through the transition to normal forward flight. Evaluations were also made of the control required to hover with and without artificial damping. Static force tests were also conducted to aid in the analysis of the flight tests. With artificial rate stabilization, very smooth transitions could be made consistently with relatively little difficulty. Because of the lower apparent damping and a tendency to diverge in yaw, however, the swept-wing configuration was considered to be much more difficult to control than the delta-wing configuration. With rate dampers off, both configurations were very difficult to control and the control power needed for satisfactory flights was substantially higher than with the rate dampers operating.

INTRODUCTION

During the early 1950's, considerable interest was expressed in vertical-attitude VTOL fighter configurations. The flight program for the delta-wing X-13 research vehicle (ref. 1) demonstrated the ability of such configurations to complete transitions between hovering and forward flight in a relatively simple, straightforward manner. VTOL fighters of this type involve less compromise of the normal forward flight configuration to accommodate VTOL operation than do the various horizontal-attitude concepts that have been studied. However, the vertical-attitude VTOL concept was not developed into an operational aircraft at that time for a number of reasons, including:

(1) The thrust required for VTOL was so much greater than that demanded by any conventional flight requirement, that the additional engine size caused unacceptable losses in the payload and range.

(2) The necessity of an elaborate ground apparatus for take-off and landing was considered operationally unacceptable.

(3) The vertical attitude of the cockpit during low-speed VTOL operations resulted in objectionable pilot attitudes which were judged to be unacceptable for an operational environment, particularly during landing.

As a result of these shortcomings, interest in the concept greatly diminished.

Recently, however, advances in fighter requirements and technology have resulted in configuration features which may minimize or even eliminate some of the previous shortcomings of vertical-attitude VTOL vehicles. For example, recent lightweight fighter prototypes have uninstalled thrust-weight ratios of about 1.5 — this level of thrust being required to meet the combat performance requirements. Also available are fly-by-wire control systems. These features suggest the possibility of a vertical-attitude VTOL fighter which is essentially a conventional airplane with conventional landing gear which can be used whenever a conventional landing is possible. Added features needed for VTOL would be a jet-reaction control system for control in hover and at low speeds, a landing hook for vertical landing on an apparatus such as that used for the X-13, and a pivoted nose-cockpit section so that the pilot could remain in a normal attitude as the airplane tilted to a vertical attitude for take-off and landing. The fly-by-wire control system would greatly facilitate this latter design feature as well as provide any particular control phasing required during the transition. In view of the foregoing considerations, it appears that a new look at the vertical-attitude VTOL fighter concept is warranted. Figure 1 shows a sketch of the concept under discussion.

The present investigation was conducted to study the dynamic stability and control characteristics of a free-flight model of vertical-attitude VTOL fighter configurations having such a pivoted fuselage forebody. The investigation was conducted in the Langley full-scale tunnel and included hovering and transition flight tests and static force tests. Since delta wings generally have good high angle-of-attack characteristics, the present investigation included a delta-wing configuration, but also included a sweptback wing in order to investigate the effects of planform. The flight tests included an investigation of: (1) stability characteristics at several attitudes during the transition from hovering to forward flight, (2) the control power used during the hover, and (3) the need for artificial rate damping.

Selected scenes from a motion picture of the free-flight tests have been prepared as a film supplement available on loan. A request card and a description of the film (L-1186) are included at the back of this report.

SYMBOLS

All static longitudinal forces and moments are referred to the wind-axis system and all static lateral-directional forces and moments are referred to the body-axis system

shown in figure 2. Static moment data for the delta-wing configuration are presented with respect to a center of gravity located at 37 percent of the wing mean aerodynamic chord and static moment data for the swept-wing configuration are presented with respect to a center of gravity located at 25 percent of the wing mean aerodynamic chord. In order to facilitate international usage of data presented, dimensional quantities are presented both in the International System of Units (SI) and in the U.S. Customary Units. Measurements were made in the U.S. Customary Units and equivalent dimensions were determined by using the conversion factors given in reference 2.

b span, m   (ft)

$\bar{c}$ mean aerodynamic chord, m   (ft)

C_D drag coefficient, $F_D/q_\infty S$

C_l rolling-moment coefficient, $M_X/q_\infty Sb$

C_L lift coefficient, $F_L/q_\infty S$

C_m pitching-moment coefficient, $M_Y/q_\infty S\bar{c}$

C_n yawing-moment coefficient, $M_Z/q_\infty Sb$

C_Y side-force coefficient, $F_Y/q_\infty S$

F_D drag force, N   (lb)

F_L lift force, N   (lb)

F_Y side force, N   (lb)

I_X moment of inertia about X body axis, kg-m^2 (slug-ft^2)

I_Y moment of inertia about Y body axis, kg-m^2 (slug-ft^2)

I_Z moment of inertia about Z body axis, kg-m^2 (slug-ft^2)

M_X rolling moment, m-N   (ft-lb)

M_Y pitching moment, m-N   (ft-lb)

M_Z yawing moment, m-N   (ft-lb)

q_∞ free-stream dynamic pressure, N/m^2 (lb/ft^2)

S wing area, m^2 (ft^2)

α angle of attack of fuselage, deg

β angle of sideslip, deg

δ_a aileron deflection (per surface), positive for left roll, deg

$\delta_{f,le}$ wing leading-edge flap deflection, positive for leading edge down, deg

δ_n forebody-deflection angle, positive for nose down from fuselage reference line (see fig. 2), deg

δ_r rudder deflection, positive for left yaw, deg

ΔC_l incremental rolling moment

ΔC_n incremental yawing moment

ΔC_Y incremental side force

$$C_{l_\beta} = \frac{\partial C_l}{\partial \beta} \qquad C_{n_\beta} = \frac{\partial C_n}{\partial \beta} \qquad C_{Y_\beta} = \frac{\partial C_Y}{\partial \beta}$$

$$C_{n_{\beta,dyn}} = C_{n_\beta} - \frac{I_Z}{I_X} C_{l_\beta} \sin \alpha$$

MODEL, APPARATUS, AND TEST TECHNIQUE

Model and Apparatus

The configurations studied were intended to represent a "wirehanger" type of VTOL configuration (similar to the X-13) which could land and take off vertically from a landing platform. In this concept, a hook located near the nose gear of the vehicle engages a

horizontal-supporting member, or wire, on the platform for launch and recovery. Following a vertical landing, the platform would be rotated to a horizontal position, and the vehicle would roll off on conventional landing gear.

In the present investigation, the landing platform was represented by a sheet of plywood, and the model-supporting member consisted of a 1.27-cm (1/2-in.) metal bar attached to the platform with brackets.

The model used in the investigation was a modified version of an existing research model generally representative of current fighter configurations. Three-view sketches of the delta- and swept-wing configurations are presented in figure 3, photographs of the model are presented in figure 4, and mass and geometric characteristics of the two configurations are presented in table I. The delta-wing configuration had leading-edge sweep of 56°. The swept-wing configuration (sweep angle of 40°) had a smaller vertical tail, and the wing incorporated leading-edge flaps which were deflected 25° for all the tests reported herein.

The entire fuselage forebody including the cockpit was pivoted to permit 90° of nose-down rotation relative to the fuselage. The pivot position was at the center of gravity of the fuselage forebody and thus pivoting the fuselage forebody did not alter the center of gravity of the complete model. The angular position of the forebody was set by a remotely controlled electric motor.

Power for thrust was obtained from compressed air which was brought into the top of the model (see fig. 4(b)) through flexible plastic tubing attached near the center of gravity. The air was fed into an ejector which exhausted out the engine nozzle exit. This propulsive arrangement was used in order to promote additional mass flow into the open engine inlet and the auxiliary engine inlets. (See fig. 3.)

The longitudinal controls consisted of an all-movable horizontal tail and a jet-reaction control mounted at the rear of the fuselage; lateral-directional controls consisted of aileron surfaces on the wing and jet-reaction controls mounted at each wing tip; and the directional controls consisted of a conventional rudder and a jet-reaction control mounted at the rear of the fuselage. The jet-reaction controls (see figs. 3 and 4(a)) were small aluminum tubes from which compressed air exhausted in response to the position of a valve operated by the control actuator. The control surfaces and the associated jet-reaction controls were interconnected such that the control surfaces moved whenever the jet-reaction controls were actuated. Thus, the control power used was a combination of the aerodynamic and jet-reaction controls. The controls were actuated by electropneumatic servos which provided a full-on or full-off flicker-type deflection. The amount of control moment produced by the jet-reaction controls could be changed by varying the pressure. Each actuator had a motor-driven trimmer which was electrically operated by

the pilots so that controls could be rapidly trimmed independently of the flicker controls. The model was equipped with individual rate-damper systems for each axis which could be turned on and off separately. The rate dampers consisted of compressed-air-driven rate gyroscopes that actuated the control servos in proportion to roll rate, yaw rate, and pitch rate. The following control surface deflections were used during the flights:

Control surface	Pilot (flicker)	Damper (proportional system, maximum deflection)
Horizontal tail, deg	±6	±3
Ailerons, deg	±6	±5
Rudder, deg.	±16	±5

Free-Flight Test Technique

The typical test setup for the free-flight tests is shown in figure 5. The model was flown without restraint in the 9- by 18-m (30- by 60-ft) open-throat test section of the Langley full-scale tunnel and remotely controlled about all three axes by human pilots. Three pilots were used during the tests. The two pilots who controlled the model about its roll and yaw axes were located in an enclosure at the rear of the test section while the third pilot, who controlled the model in pitch, was stationed at one side of the tunnel. Operators were also stationed at the side of the tunnel to control the model power, safety cable, and the forebody-deflection angle. Pneumatic and electric power and control signals were supplied to the model through a flexible trailing cable which was made up of wires and light plastic tubes. The cable also incorporated a 0.318-cm (1/8-in.) steel cable that passed through a pulley above the test section. This element of the flight cable was used to restrain the model when an uncontrollable motion or mechanical failure occurred. The entire flight cable was kept slack during the flights by a safety-cable operator using a high-speed pneumatic winch. A further discussion of the free-flight technique, including the reasons for dividing the piloting tasks, is given in reference 3.

TESTS

Free-Flight Tests

The investigation consisted of free-flight tests to study the dynamic stability and control characteristics of the delta-wing and swept-wing configurations over the speed range from hovering to forward flight. The flights began with a vertical take-off from the landing platform, included a transition wherein the cockpit remained essentially horizontal

until $\alpha \approx 30^O$, and ended with the model in conventional forward flight at high angles of attack (minimum $\alpha = 25^O$) with $\delta_n = 0^O$. The tests included steady flights at several attitudes, an examination of the control power used, and an evaluation of the need for artificial rate damping. The results of the flight tests were mainly qualitative and consisted of pilot opinions of the overall behavior of the model.

Motion-picture records were made of all flights and selected scenes are included in a film supplement to this paper.

Force Tests

Static force tests were conducted in the Langley full-scale tunnel at a Reynolds number of about 1.64×10^6 per meter (0.5×10^6 per foot). These tests were made to determine the aerodynamic characteristics of the model and to determine values of static stability derivatives for use in the analysis and interpretation of the free-flight tests. The forebody-deflection angle δ_n was varied from 0° (alined with fuselage reference line) to 90° (perpendicular to fuselage reference line) in increments of $\delta_n = 10^O$. At each forebody-deflection angle, tests were made over an angle-of-attack range as follows:

δ_n, deg	α range, deg
0	0 to 20
10	0 to 20
20	10 to 20
30	20 to 40
40	30 to 50
50	40 to 60
60	50 to 70
70	60 to 80
80	70 to 90
90	80 to 100

Note that the middle angle of attack of each range (except for $\delta_n = 0^O$) is where $\alpha = \delta_n$. As a result, the local angle of attack at the nose was 0°. Thus, the test condition represented a point during a level-flight transition. The range of angle of attack was then repeated for the various angles of sideslip from -5° to 5°. Tests were also conducted to determine the aileron and rudder effectiveness of the two configurations for angles of attack from 0° to 100° with forebody deflection of both 0° and 90° ($\beta = 0^O$).

The forces and moments were measured on a six-component, internal, strain-gage balance and the model was mounted on a strut that entered the top of the fuselage just behind the center of gravity.

Conventional wind-tunnel corrections for flow angularity have been applied to all force-test data presented herein. No wall corrections were applied because of the very small size of the model relative to that of the tunnel test section.

RESULTS OF FORCE TESTS

Static Longitudinal Stability

The static longitudinal stability characteristics of the model are presented in figure 6 for the delta- and swept-wing configurations. The data indicate that the swept-wing configuration exhibited a higher value of maximum lift. The data also show that both configurations were longitudinally stable over the test range of angle of attack and that deflecting the nose over the range indicated had little effect on the static longitudinal characteristics. The stability was subsequently verified in the free-flight tests.

Static Lateral-Directional Stability

The static lateral-directional stability derivatives $\left(C_{Y_\beta}, \ C_{n_\beta}, \text{ and } \ C_{l_\beta} \right)$ of the delta- and swept-wing configurations are presented in figure 7. The values of the derivatives were based on measurements obtained for an angle-of-sideslip range of $\pm 5^O$. The solid symbols in figure 7 correspond to test conditions which represent a level-flight transition with a horizontal cockpit attitude ($\alpha = \delta_n$).

The data of figure 7(a) show that the delta-wing configuration had a relatively large positive (stable) value of C_{n_β} at low angles of attack, but at angles of attack above about 25°, the directional stability became very unstable. Data also show that the forebody-deflection angle had a significant effect on directional stability. For example, the value of C_{n_β} at $\alpha = 60^O$ was stable for $\delta_n = 50^O$ and unstable for $\delta_n = 70^O$. In addition, the magnitude of the effective dihedral derivative C_{l_β} was very sensitive to forebody-deflection angle in the region of maximum lift.

The data of figure 7(b) show that similar trends existed for the swept-wing configurations, however, the unstable values of C_{n_β} near maximum lift were much larger than those of the delta-wing configuration. In addition, near maximum lift, there was a very rapid decrease in the value of effective dihedral from a large stable (negative) quantity to a neutral (zero) or slightly unstable (positive) quantity. The loss of effective dihedral together with loss of static directional stability at high angles of attack can promote directional divergence as discussed in reference 4.

Lateral-Directional Control Characteristics

The results of the tests to determine the aerodynamic control effectiveness of the rudder and ailerons for the two configurations are presented in figures 8 and 9. The data are presented as the incremental values of C_l, C_n, and C_Y produced by a right-yaw or right-roll control.

Figure 8 shows the incremental forces and moments produced by rudder deflection for a right-yaw control. The data show that the effectiveness of the rudder was fairly constant up to $\alpha = 30^O$. Above $\alpha = 30^O$ the effectiveness decreased markedly, and the rudder effectiveness of both configurations was about zero at angles of attack greater than $\alpha = 50^O$. No change of rudder effectiveness due to forebody deflection can be seen.

Shown in figure 9 are the values of ΔC_Y, ΔC_n, and ΔC_l produced by aileron deflection for right-roll control. The data show that the effectiveness of the ailerons decreased with increasing angle of attack. In addition, the data show that aileron deflection produced large values of adverse yawing moment near $\alpha = 60^O$. No change in aileron effectiveness due to forebody deflection is apparent.

RESULTS AND DISCUSSION OF THE FLIGHT TESTS

All the free-flight tests were made for a center of gravity located at $0.37\bar{c}$ for the delta-wing configuration and $0.25\bar{c}$ for the swept-wing configuration. A motion-picture film supplement with selected scenes from the free-flight tests has been prepared and is available on loan. A request form and a description of the film are included at the back of this paper.

Longitudinal Characteristics

As mentioned previously, most of the tests were made as continuous flights from hover to normal forward flight (minimum $\alpha = 25^O$). Without artificial rate damping, flights could be made from hover to normal forward flight with no significant problem to the pitch pilot except for the normal necessity of maintaining a very careful attention to the change of trim through the transition. Both model configurations were neutrally stable in hovering flight. Without the artificial rate damping, it was necessary to use high levels of control power for a smooth flight. Therefore, almost all the flights were made with the rate dampers on because of the difficulty of obtaining a smooth hover and entry into the transition and the need to greatly reduce the pilot's control effort and control power. The longitudinal stability and control characteristics of both configurations were satisfactory, as would be expected based on the results of the force tests.

Lateral-Directional Characteristics

Delta-wing configuration.- With roll and yaw rate dampers off, it was very difficult for the roll and yaw pilots to control the delta-wing configuration through the transition from hovering to normal forward flight. In addition to neutral stability in hover, the delta-wing configuration experienced large rolling and yawing motions midway through the transition. With the roll and yaw rate dampers on, however, it was possible to make consistently good transitions from hover to normal forward flight and the model motions were smooth and easy to control.

Swept-wing configuration.- With roll and yaw rate dampers off, the swept-wing configuration was even more difficult to control than the delta-wing configuration. It was the pilots' opinion that the swept-wing configuration was much more lightly damped than the delta-wing configuration and it displayed a definite tendency to diverge in yaw in the higher speed portion of the transition range. With the roll and yaw rate dampers on, the swept-wing configuration became much easier to control and the pilots were able to make fairly smooth transitions. Even with the artificial rate damping on, the tendency of the swept-wing configuration to diverge in yaw was still noticeable. The pilots, therefore, considered the swept-wing configuration more difficult to control than the delta-wing configuration.

The tendency of the swept-wing configuration to diverge in yaw can be predicted based on a criterion known as $C_{n_{\beta},dyn}$ which has been used in past investigations to evaluate the effects of lateral and directional stability, angle of attack, and inertial distribution on dynamic stability. In particular, the past studies have shown that negative values of $C_{n_{\beta},dyn}$ indicate the tendency toward divergence in yaw where

$$C_{n_{\beta},dyn} = C_{n_{\beta}} - \frac{I_Z}{I_X} C_{l_{\beta}} \sin \alpha$$

The values of $C_{n_{\beta},dyn}$ are presented in figure 10 for the delta- and swept-wing configurations based on the force-test data presented in figure 7. The data show that $C_{n_{\beta},dyn}$ for the swept-wing configuration reached large negative values near $\alpha = 40^O$ (indicating the possibility of a divergence) because of the large unstable values of $C_{n_{\beta}}$ and $C_{l_{\beta}}$ indicated in figure 7(b). In contrast to the data for the swept-wing configuration, the values of $C_{n_{\beta},dyn}$ for the delta-wing configuration remained positive over the angle-of-attack range, primarily as a result of large stable values of $C_{l_{\beta}}$ as shown in figure 7(a).

Evaluation of Control Power Required in Hover

It is recognized that the minimum control power needed to control the model in hover using the free-flight-model technique would probably not correspond to minimum control power required by a pilot of a full-scale airplane due to the remote model-pilot location and rapidity of model motions. Therefore no attempt has been made to correlate the values of control power required to fly the model with values recommended for satisfactory handling qualities of a full-scale airplane. However, the values of minimum control power (scaled up to full scale) required by the pilots to maintain control of the model in hovering flight are shown in the following table. The values, which are presented in relation to the axis system perceived by the on-board pilot seated in the horizontal forebody, were obtained from calibrations of the jet-reaction controls using the minimum air-pressure level determined in the tests and were then scaled up to full scale based on an aircraft weight of 75 620 N (17 000 lb).

Parameter	Delta-wing configuration with dampers −		Swept-wing configuration with dampers −	
	Off	On	Off	On
$\dfrac{\text{Roll-control moment}}{\text{Inertia}}$, rad/sec^2	0.28	0.14	0.30	0.15
$\dfrac{\text{Yaw-control moment}}{\text{Inertia}}$, rad/sec^2	.71	.16	.68	.15

The data in the table show that with the rate dampers off, the control power needed for satisfactory flights was substantially higher than with the rate dampers operating. It is quite probable that the amount of jet-reaction control could have been reduced as the transition from hovering to normal forward flight progressed, but no attempt was made to determine the minimum control power needed at each angle of attack.

More sophisticated analysis techniques, such as piloted simulation, are required to obtain quantitative information on the flying qualities and control power required for a full-scale configuration. In addition, critical operational maneuvers, such as the vertical landing, were considered to be beyond the scope of the present study.

SUMMARY OF RESULTS

The results of a free-flight model investigation to study the dynamic stability and control characteristics of a vertical-attitude VTOL fighter airplane with a pivoted nose-cockpit design may be summarized as follows:

1. In hovering flight, the models were neutrally stable and quite sensitive to control inputs, but very smooth flights could be made using artificial rate stabilization.

2. The model exhibited satisfactory longitudinal stability in all flight tests.

3. With artificial rate dampers operating, very smooth transitions could be made consistently from hovering to normal forward flight with relatively little difficulty. Because of the lower apparent damping and a tendency to diverge in yaw, however, the swept-wing configuration was considered to be much more difficult to control than the delta-wing configuration.

4. Without artificial stabilization, both the delta-wing configuration and the swept-wing configuration were very difficult to control and the delta-wing configuration experienced large rolling and yawing motions.

5. With the rate dampers off, the control power needed by the roll and yaw pilots for satisfactory flights was substantially higher than with the rate dampers operating.

Langley Research Center
National Aeronautics and Space Administration
Hampton, Va. 23665
July 30, 1975

REFERENCES

1. Smith, Charles C., Jr.: Hovering and Transition Flight Tests of a 1/5-Scale Model of a Jet-Powered Vertical-Attitude VTOL Research Airplane. NASA TN D-404, 1961. (Supersedes NASA MEMO 10-27-58L.)

2. Mechtly, E. A.: The International System of Units - Physical Constants and Conversion Factors (Second Revision). NASA SP-7012, 1973.

3. Parlett, Lysle P.; and Kirby, Robert H.: Test Techniques Used by NASA for Investigating Dynamic Stability Characteristics of V/STOL Models. J. Aircraft, vol. 1, no. 5, Sept.-Oct. 1964, pp. 260-266.

4. Chambers, Joseph R.; and Anglin, Ernie L.: Analysis of Lateral-Directional Stability Characteristics of a Twin-Jet Fighter Airplane at High Angles of Attack. NASA TN D-5361, 1969.

TABLE I.- MASS AND GEOMETRIC CHARACTERISTICS

	Delta wing	Swept wing
Weight, N (lb)	263.56 (59.25)	252.44 (56.75)
Moments of inertia:		
I_X, kg-m^2 (slug-ft^2)	0.656 (0.484)	0.690 (0.509)
I_Y, kg-m^2 (slug-ft^2)	4.871 (3.593)	4.730 (3.489)
I_Z, kg-m^2 (slug-ft^2)	5.234 (3.861)	5.016 (3.700)
Overall fuselage length, m (ft)	2.06 (6.78)	2.06 (6.78)
Wing:		
Span, m (ft)	1.33 (4.35)	1.33 (4.35)
Area, m^2 (ft^2)	0.76 (8.20)	0.59 (6.30)
Root chord, m (ft).	0.99 (3.25)	0.72 (2.36)
Tip chord, m (ft)	0.14 (0.47)	0.14 (0.47)
Mean aerodynamic chord, m (ft)	0.68 (2.22)	0.50 (1.64)
Aspect ratio	2.31	3.00
Taper ratio	0.15	0.23
Sweepback of leading edge, deg	56	40
Dihedral, deg	0	0
Incidence, deg	0	0
Airfoil section	Modified NACA 64A204	NACA 64A204
Aileron area, m^2 (ft^2)	0.06 (0.64)	0.06 (0.64)
Leading-edge flap area, m^2 (ft^2)	----------	0.07 (0.76)
Vertical tail:	Large	Small
Area, m^2 (ft^2)	0.15 (1.59)	0.11 (1.23)
Span, m (ft)	0.38 (1.26)	0.38 (1.26)
Taper ratio	0.30	0.44
Root chord, m (ft)	0.59 (1.94)	0.41 (1.35)
Tip chord, m (ft)	0.18 (0.59)	0.18 (0.59)
Sweepback of leading edge, deg	56	47.5
Airfoil section:		
Root chord	Modified 5.3% biconvex	5.3% biconvex
Tip chord	Modified 3.0% biconvex	3.0% biconvex
Rudder area, m^2 (ft^2)	0.02 (0.26)	0.02 (0.26)
Tail length, $0.25\bar{c}$ wing to $0.25\bar{c}$ tail, m (ft)	0.47 (1.53)	0.64 (2.10)

TABLE I.- Concluded.

Horizontal tail:
  Area, m^2 (ft^2) 0.22 (2.36)
  Movable area (one side), m^2 (ft^2) 0.05 (0.49)
  Span, m (ft) 0.80 (2.62)
  Aspect ratio 3.19
  Taper ratio 0.20
  Sweepback of leading edge, deg 40
  Dihedral, deg . . . . -10
  Root chord (at model center line), m (ft) 0.42 (1.37)
  Tip chord, m (ft) 0.09 (0.28)
  Airfoil section:
    Root chord . . . . 6.0% biconvex
    Tip chord . . . . 3.5% biconvex
  Hinge-line location, percent tail chord 0.25
  Tail length, from $0.25\overline{c}$ wing to $0.25\overline{c}$ tail, m (ft) 0.72 (2.35)

Ventral fin (swept-wing configuration only):
  Area, m^2 (ft^2) 0.02 (0.16)
  Span, m (ft) 0.09 (0.29)
  Aspect ratio 0.36
  Taper ratio 0.69
  Sweepback of leading edge, deg 45
  Dihedral (cant), deg . . . . 15 outboard
  Airfoil section:
    Root chord . . . . 3.0% biconvex
    Tip chord . . . . Constant 0.02 radius
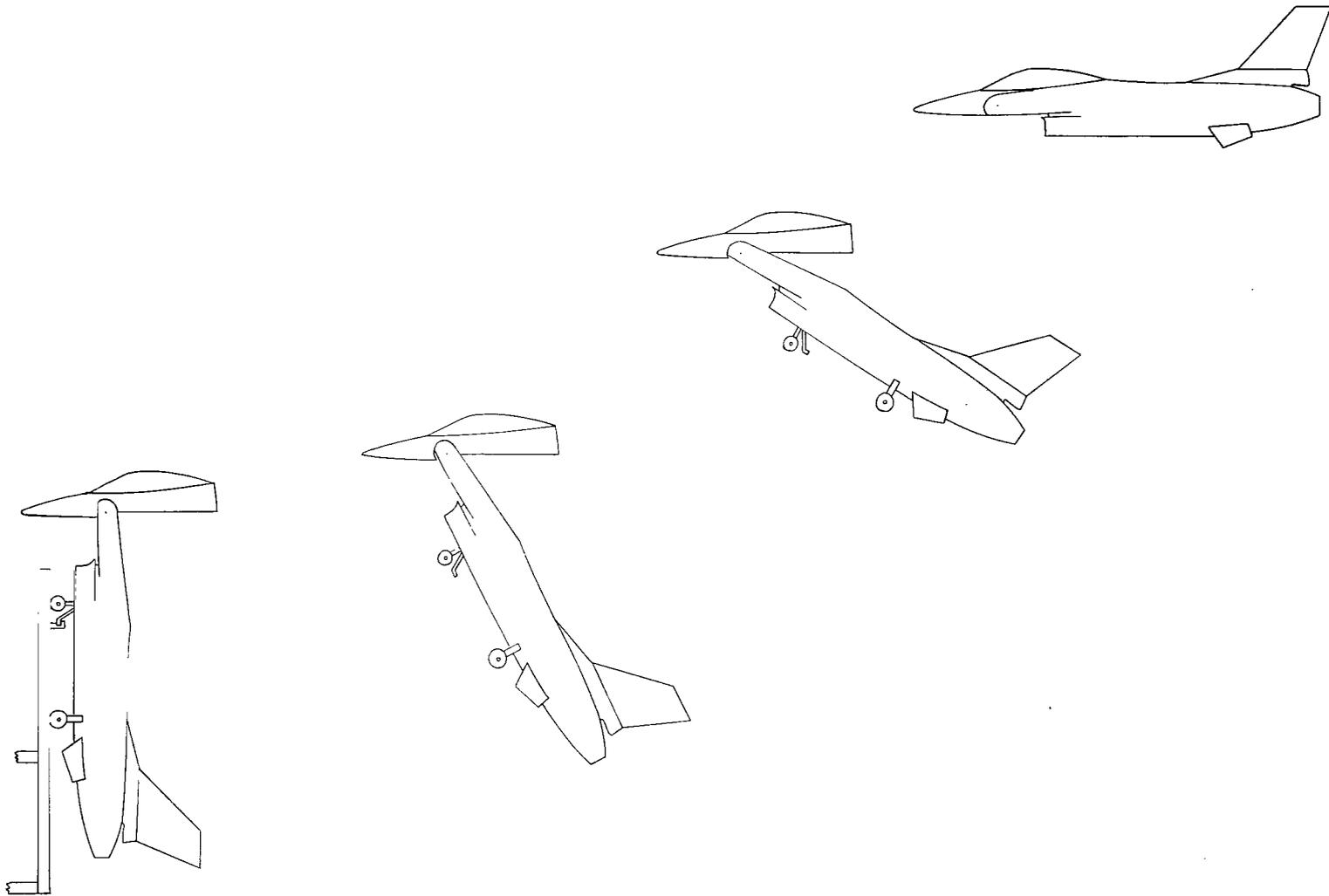
Figure 1.- Vertical-attitude VTOL fighter concept.
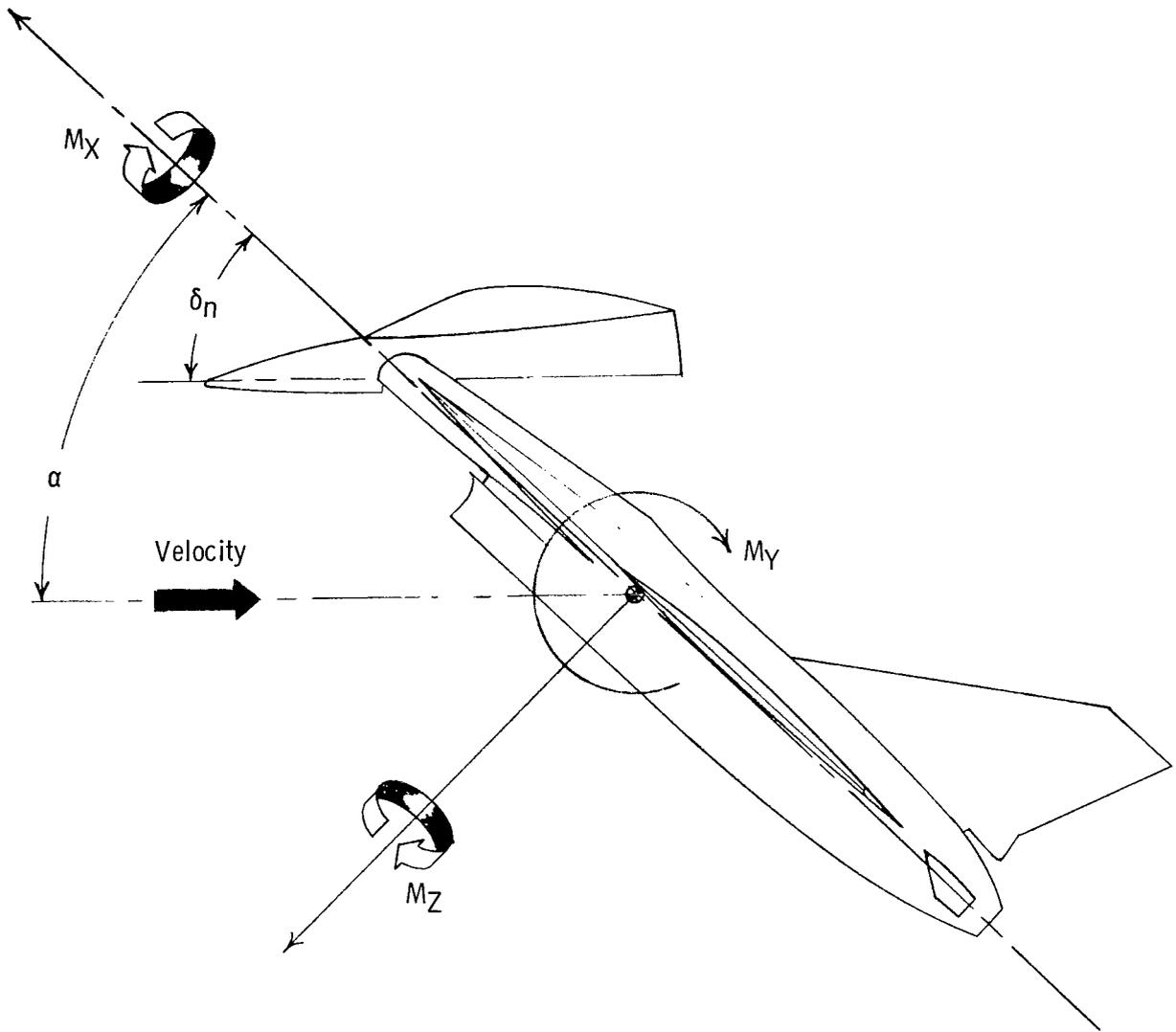
Figure 2.- Body-axis system.

Jet-reaction
controls

Swept-wing configuration

Delta-wing configuration

Nose pivot

1.33
(4.35)

2.06
(6.78)

Landing hook

Auxiliary intake
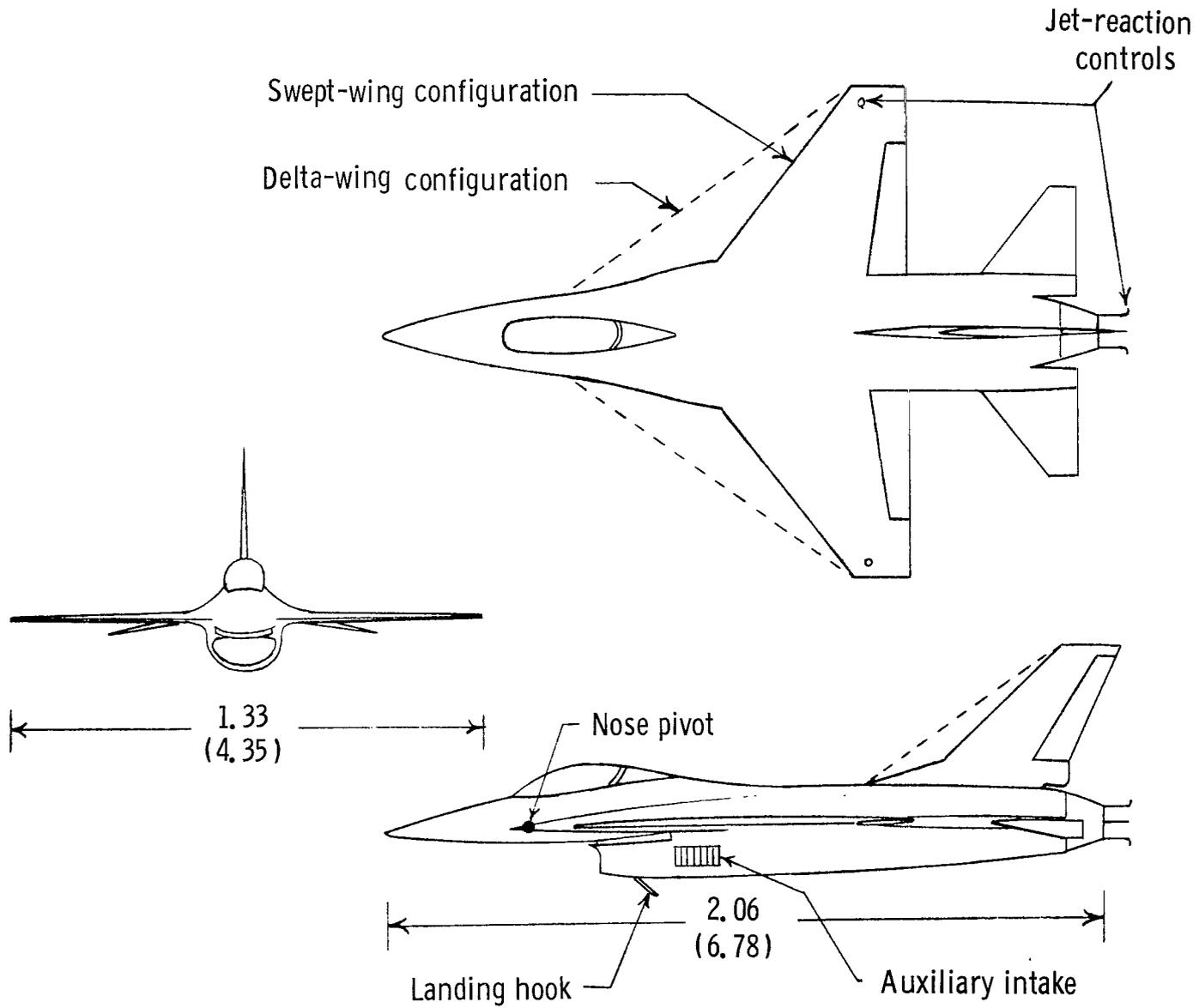
Figure 3.- Three-view sketch of the model. Dimensions are in meters (feet).
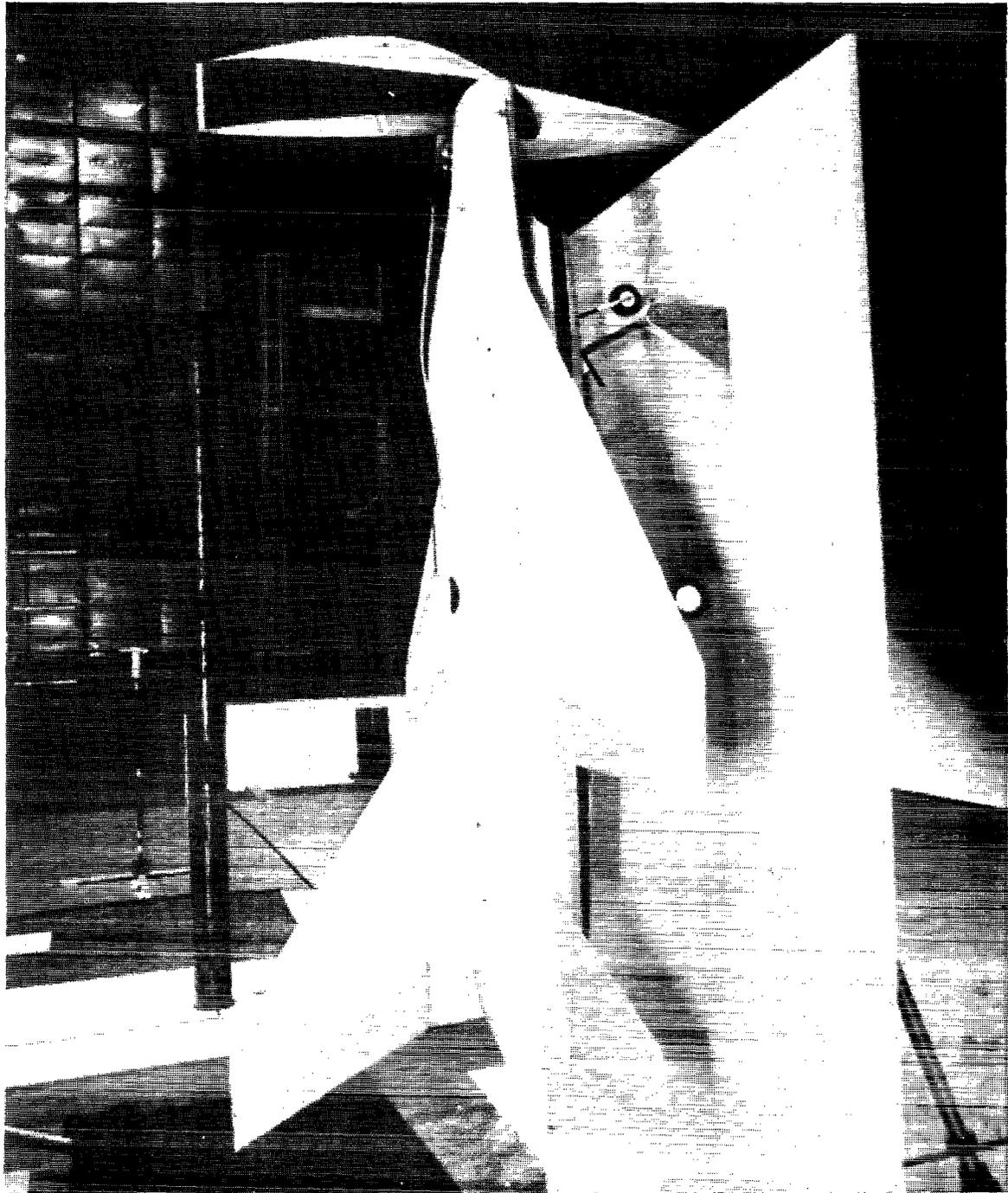
L-74-6089

(a) Hanging on take-off and landing rig.

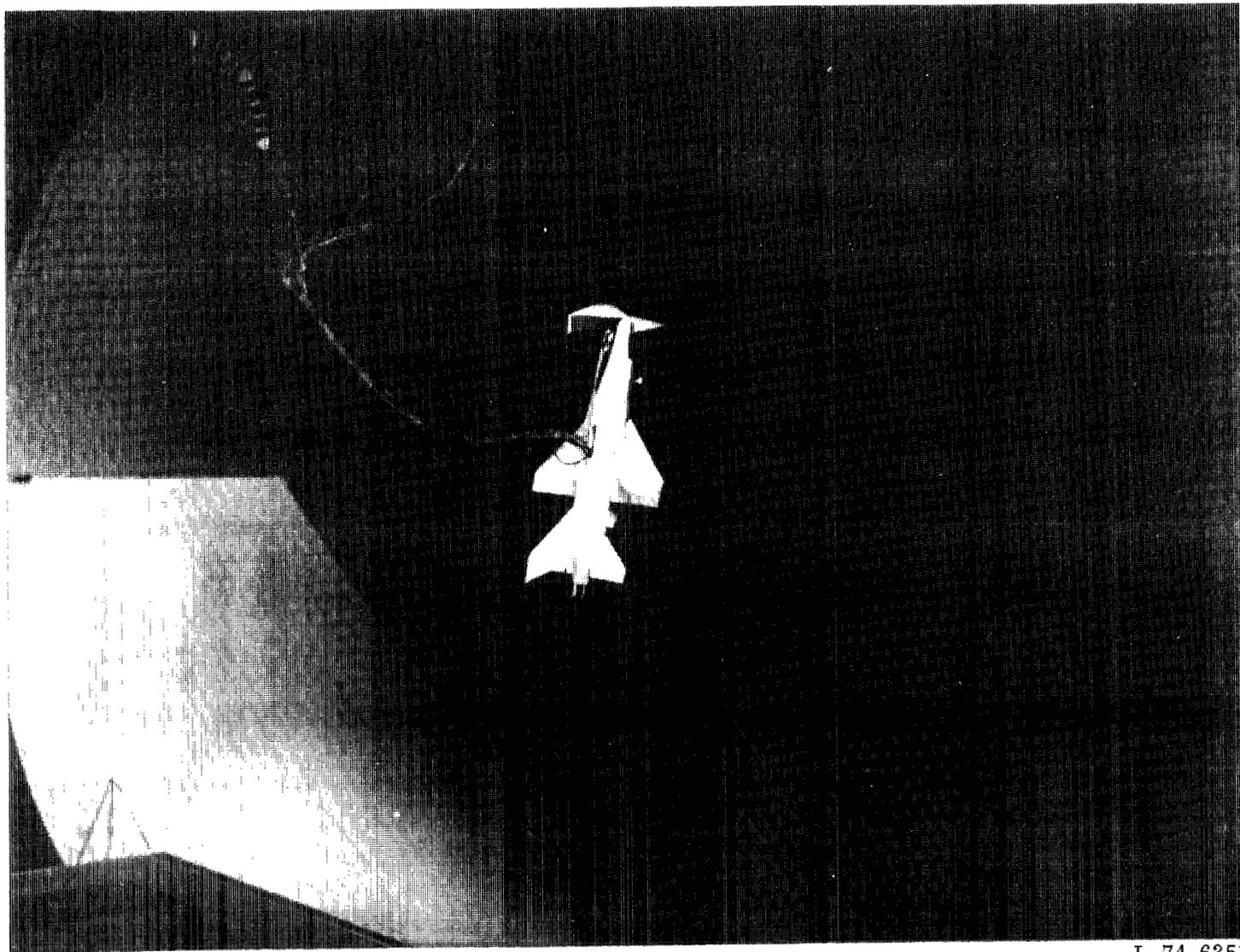Figure 4.- Model used in the tests.
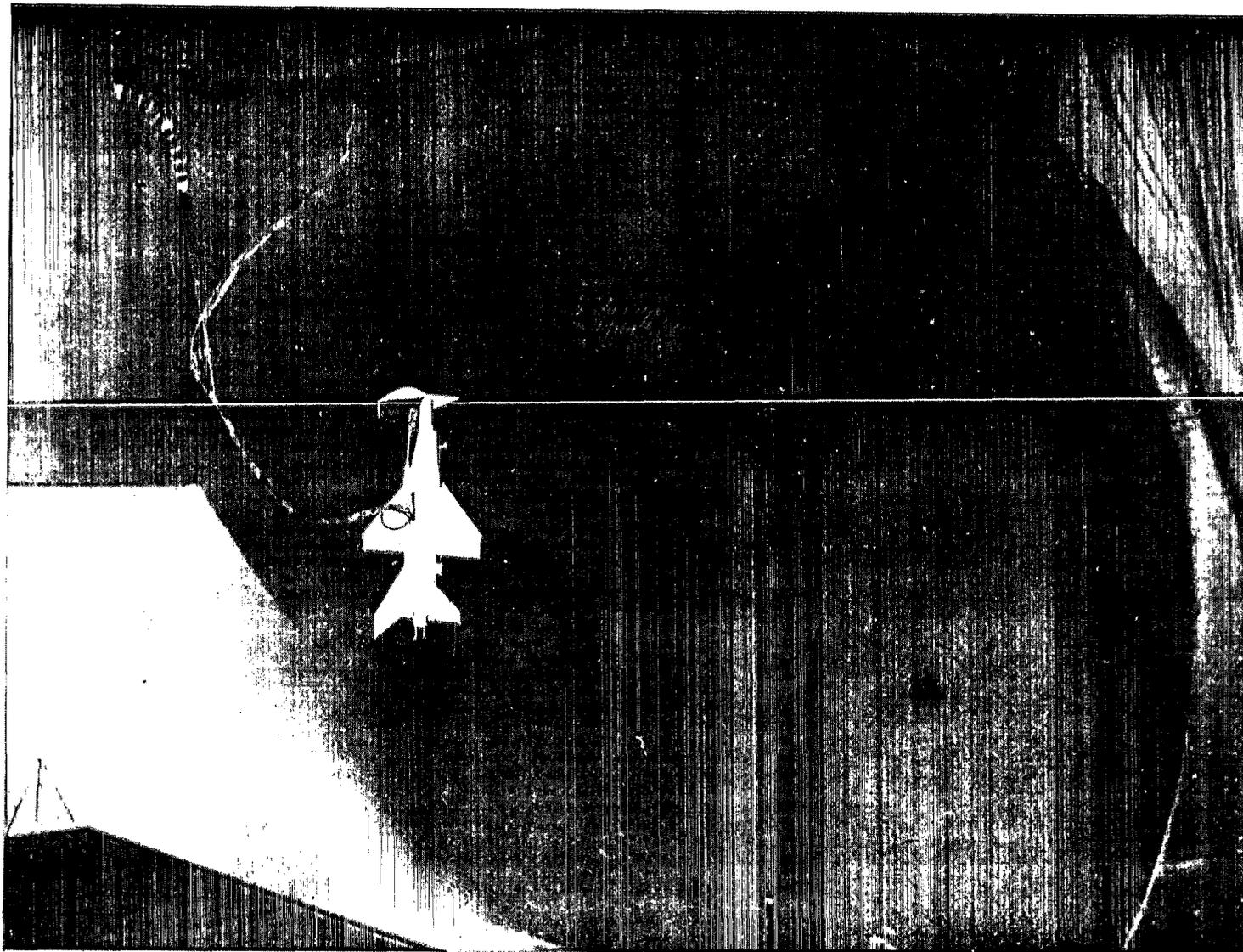
L-74-6349

(b) Hovering in full-scale tunnel.
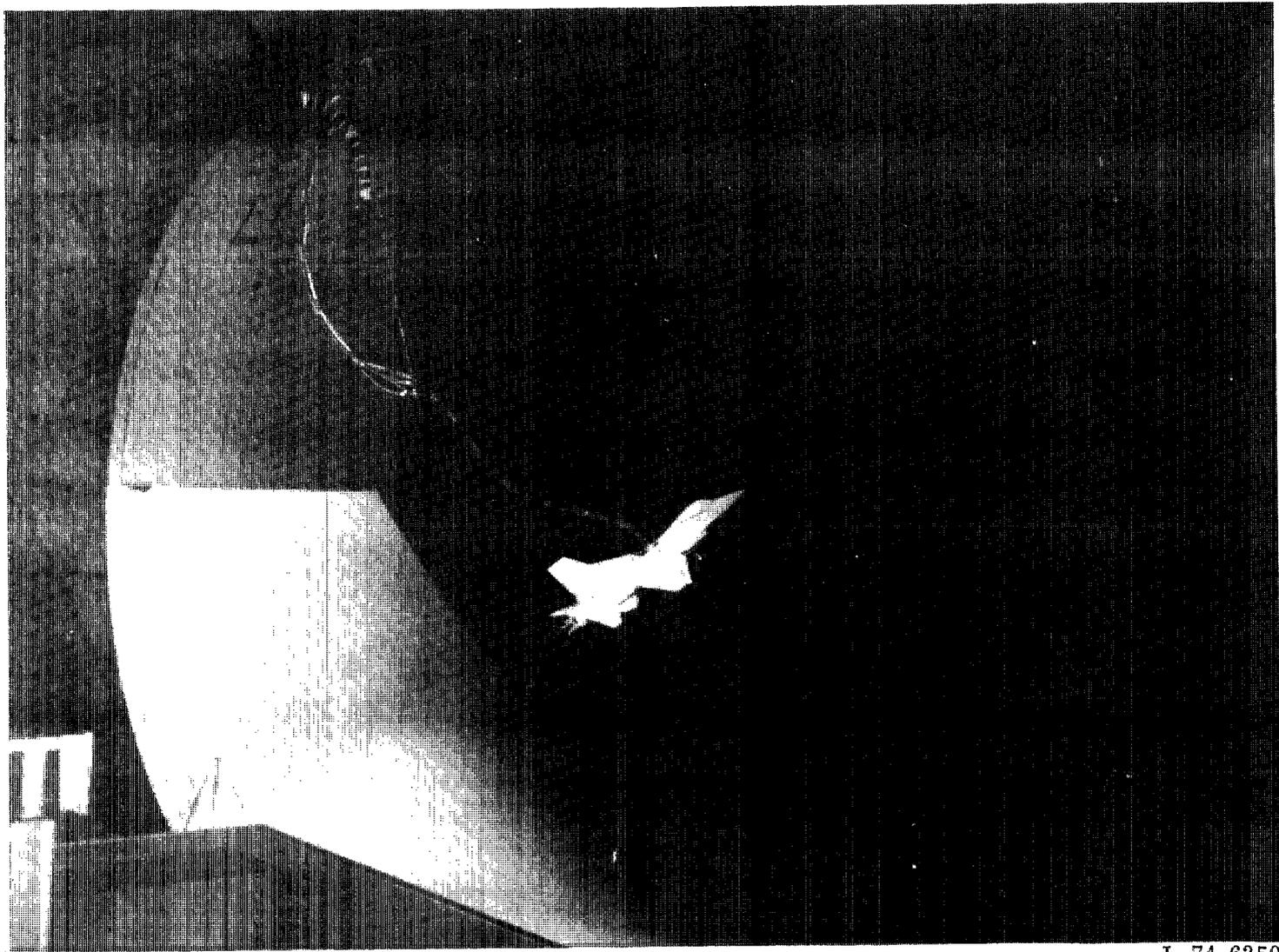
Figure 4.- Continued.

L-74-6351

(c) Start of transition.

Figure 4.- Continued.

L-74-6352

(d) Midway through the transition.

Figure 4.- Continued.

L-74-6350

(e) Normal forward flight.

Figure 4.- Concluded.

POWER AND CONTROL CABLE

SAFETY CABLE

ROLL AND YAW PILOTS

TUNNEL GROUND BOARD

SAFETY-CABLE OPERATOR

POWER OPERATOR

PITCH PILOT
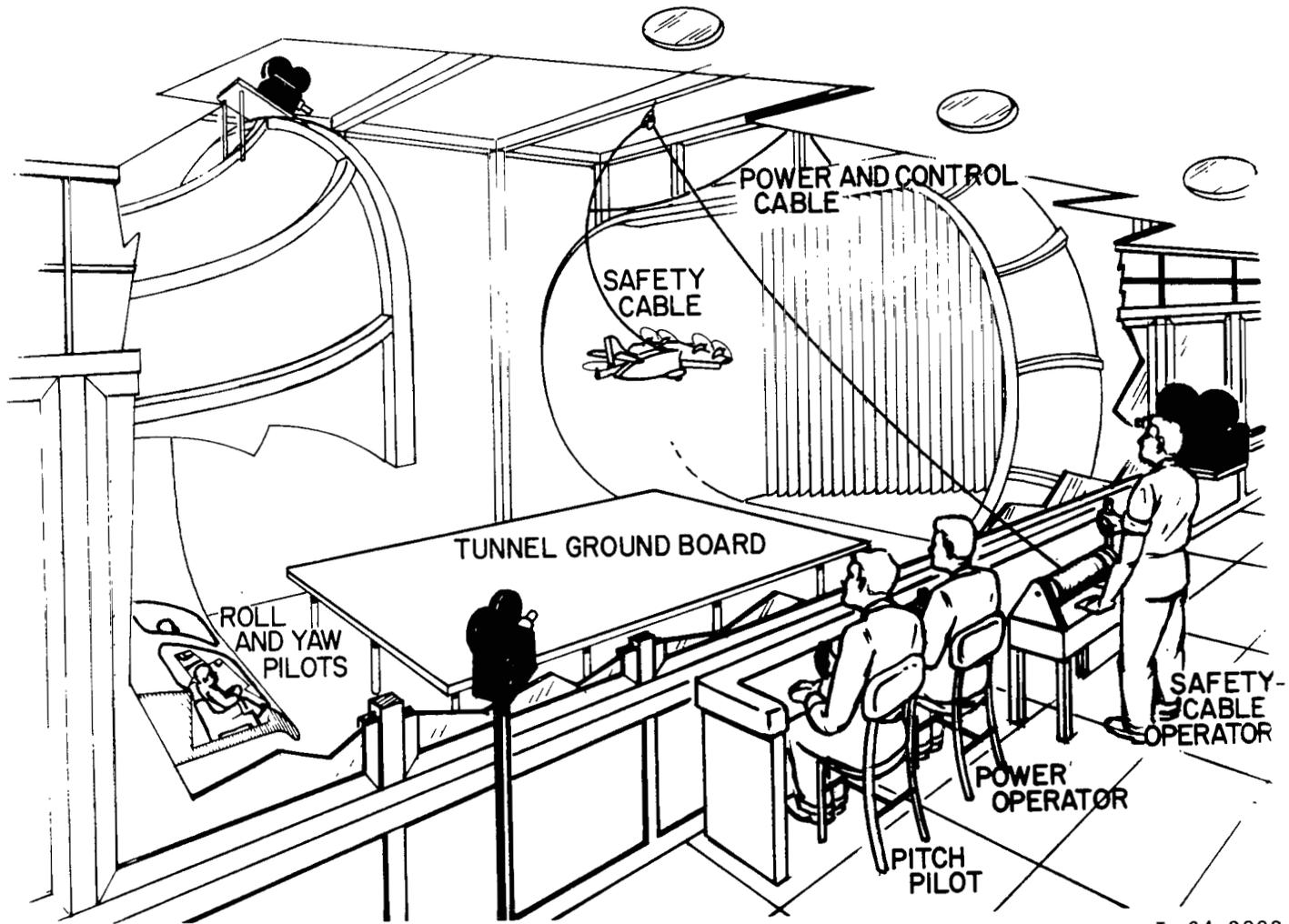
L-64-3008

Figure 5.- Typical setup for flight tests in the Langley full-scale tunnel.
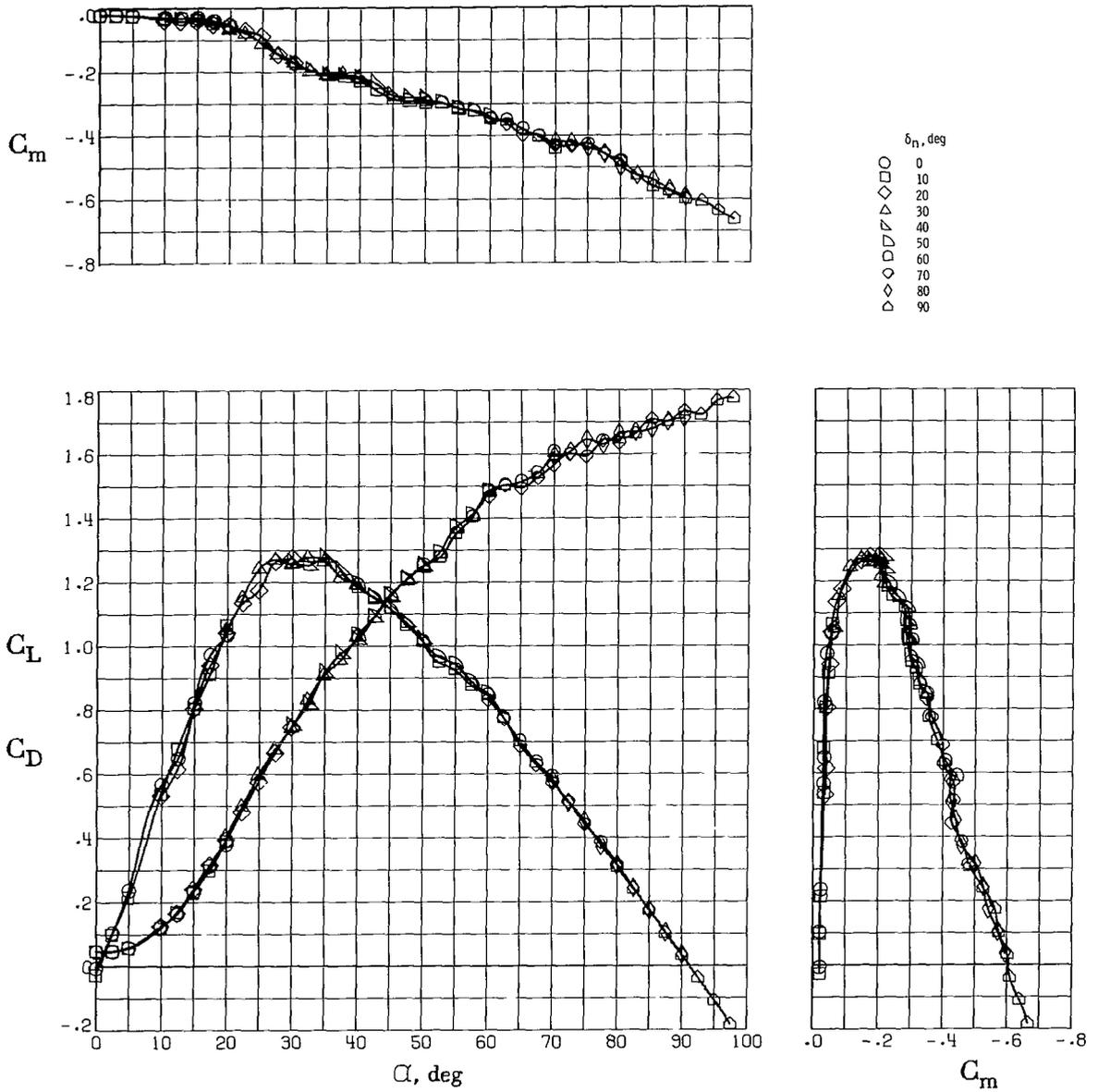
(a) Delta-wing configuration.

Figure 6.- Variation of static longitudinal characteristics.
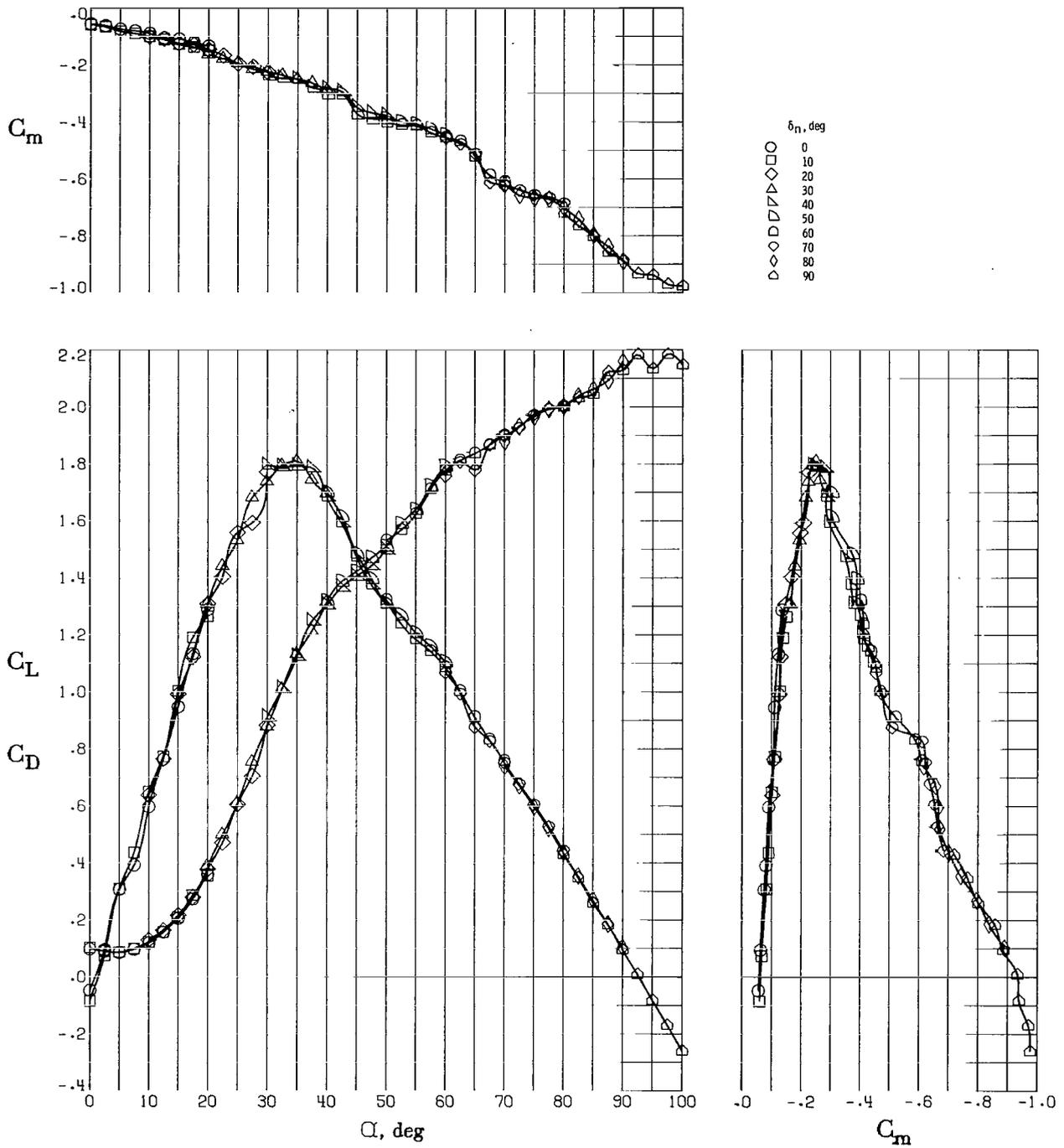
(b) Swept-wing configuration. $\delta_{f,le} = 25^{O}$.

Figure 6.- Concluded.
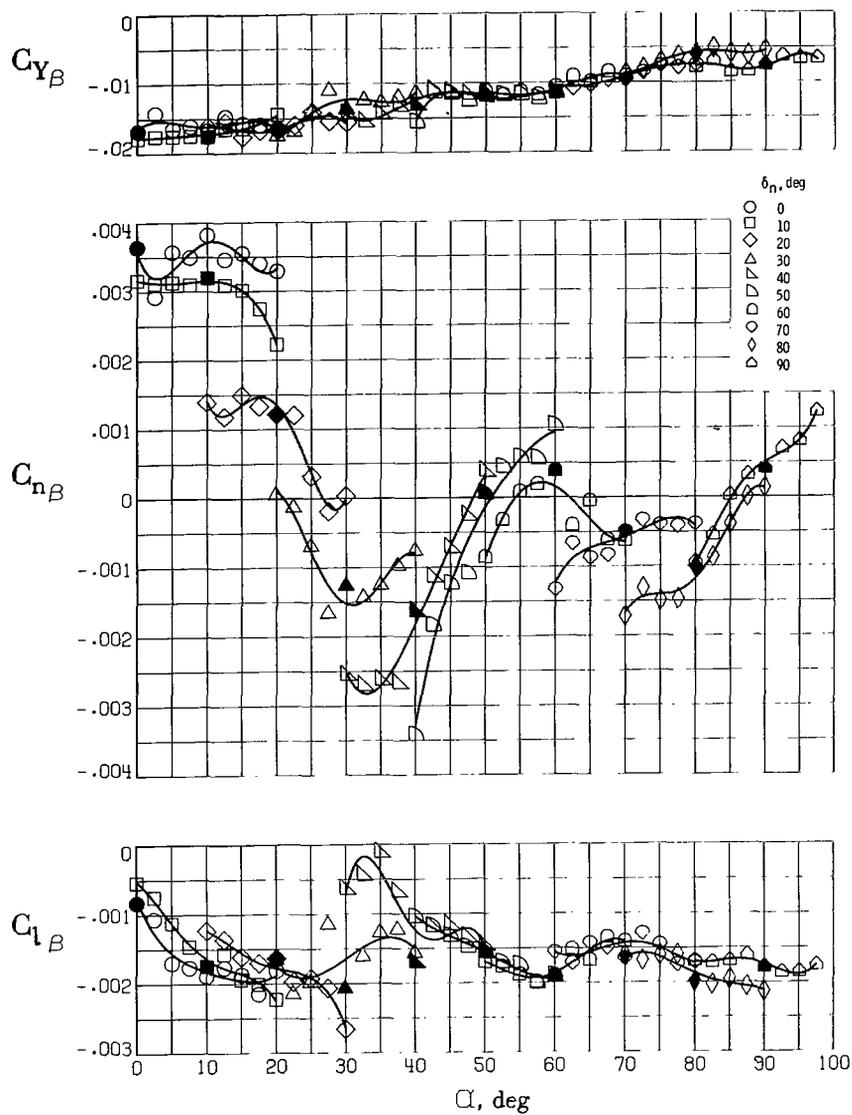
(a) Delta-wing configuration.

Figure 7.- Variation of static lateral-directional characteristics. Solid symbols correspond to test conditions which represent a level-flight transition with a horizontal cockpit attitude ($\alpha = \delta_n$).
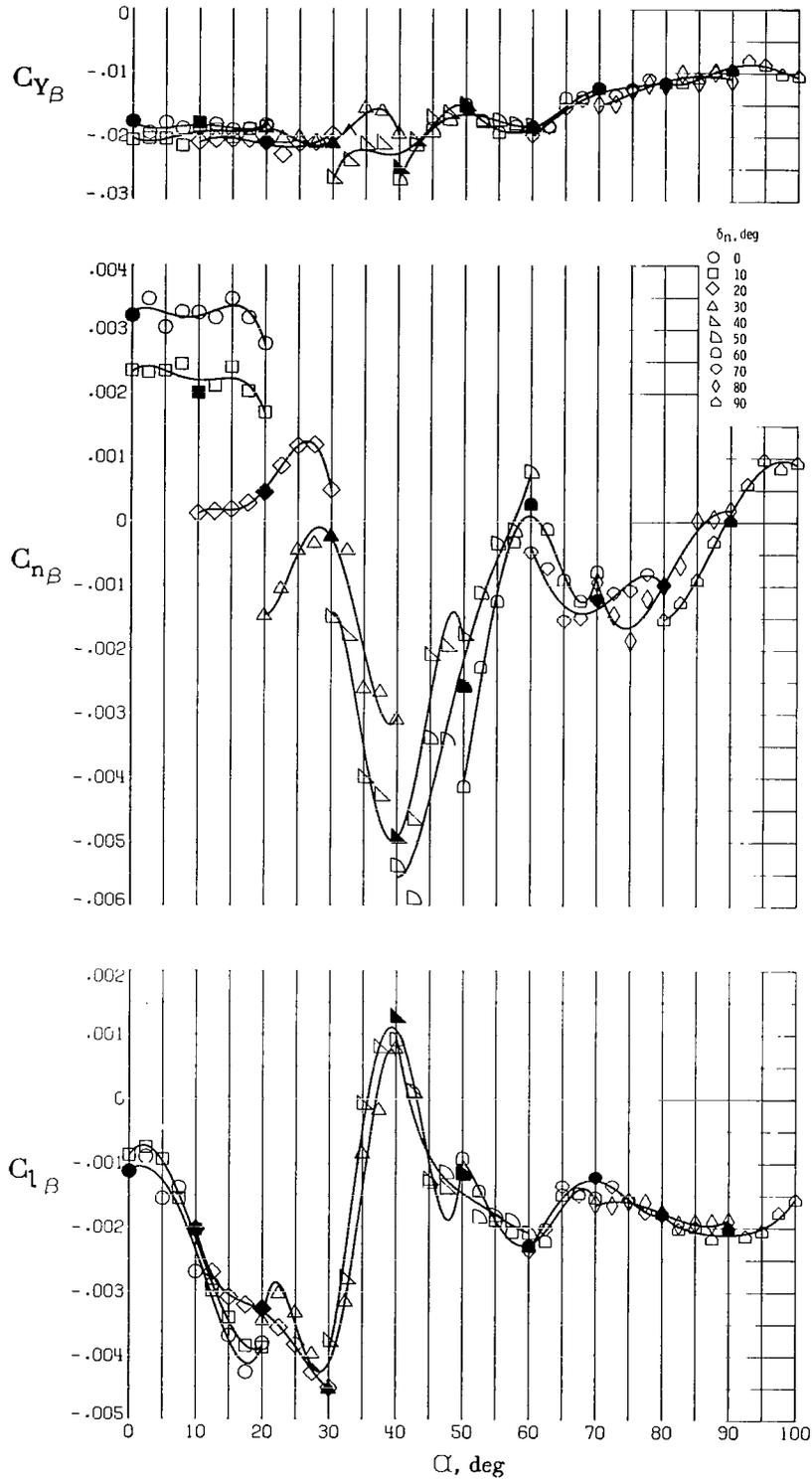
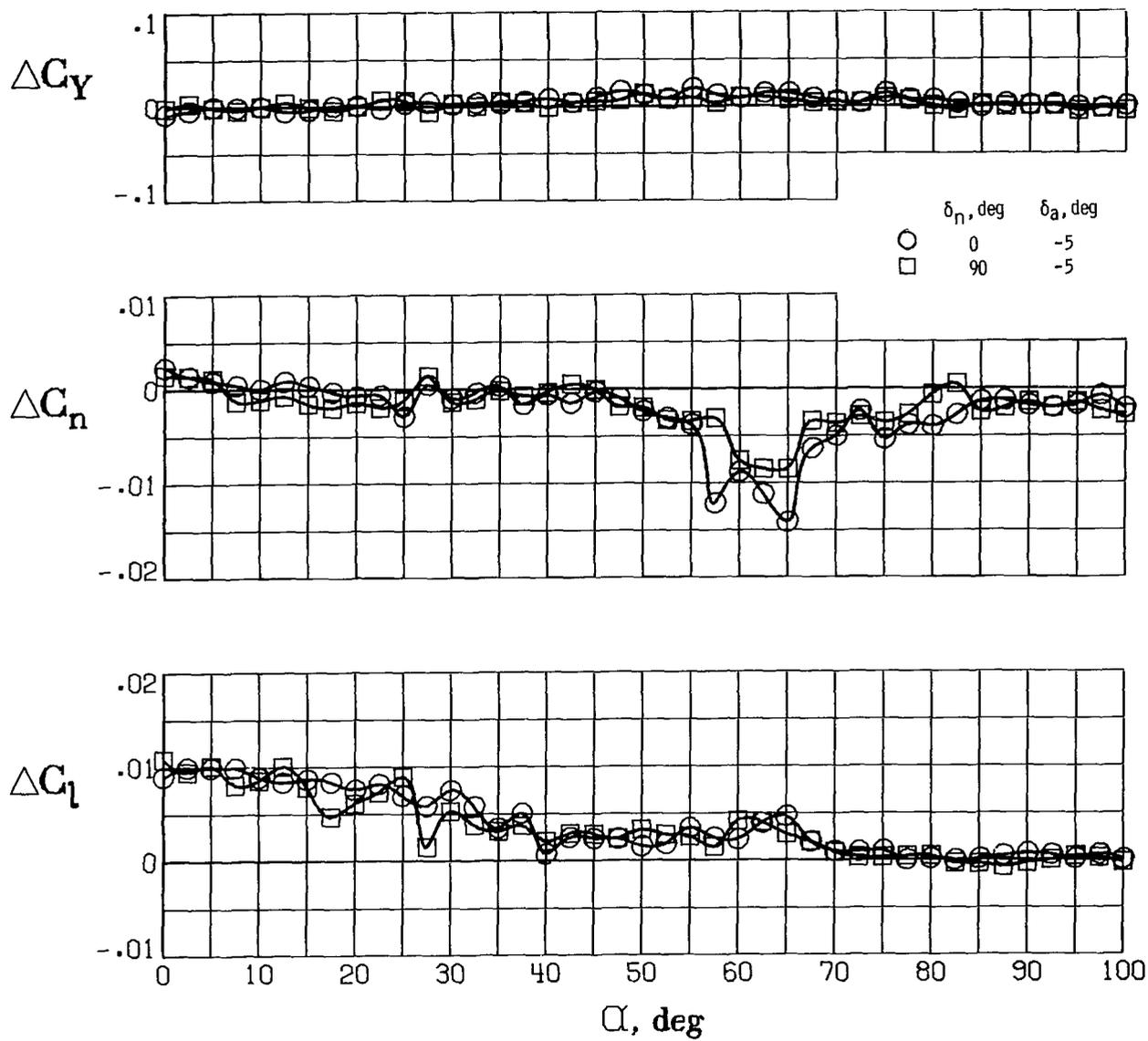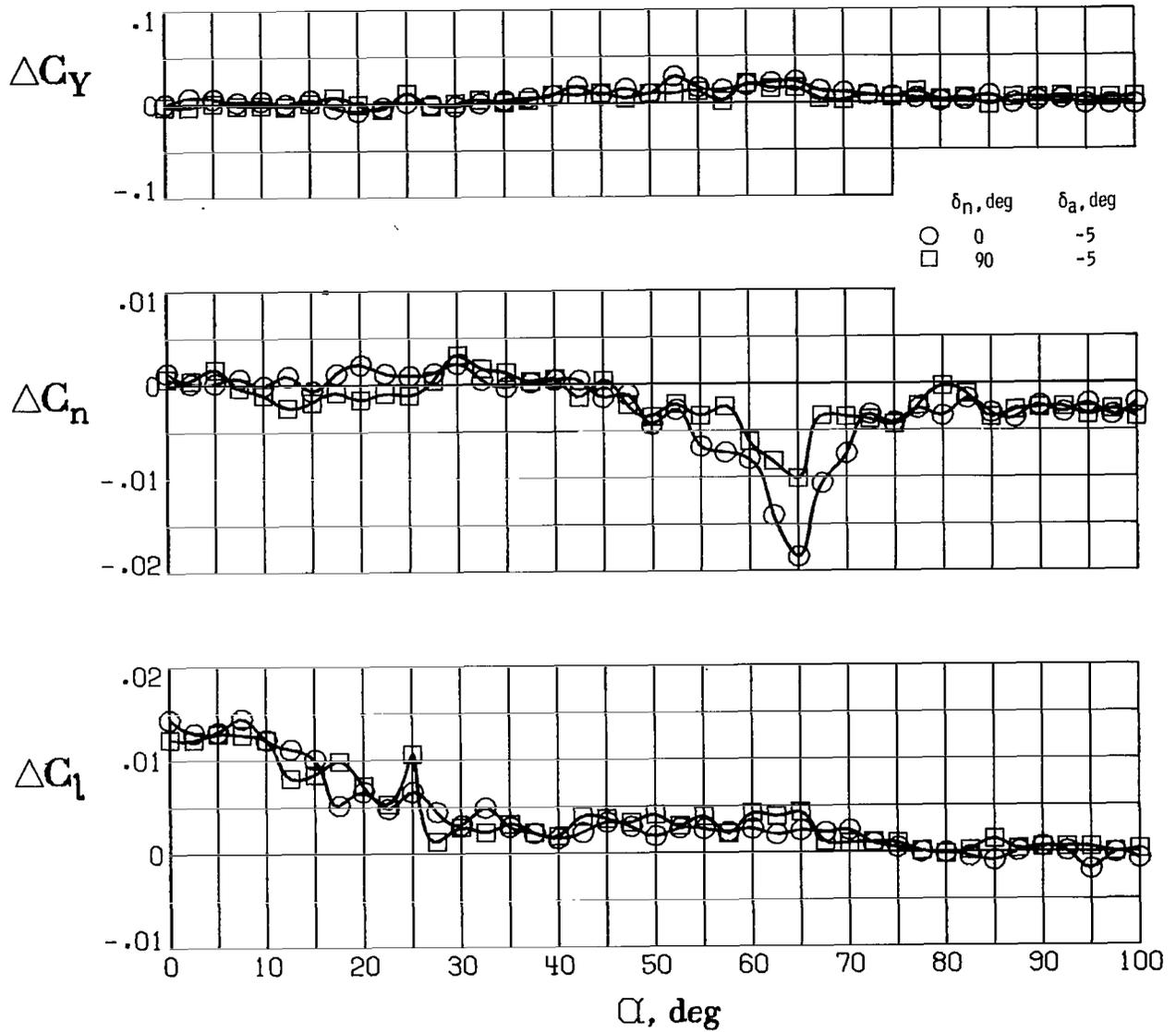(b) Swept-wing configuration. $\delta_{f,le} = 25^o$.

Figure 7.- Concluded.
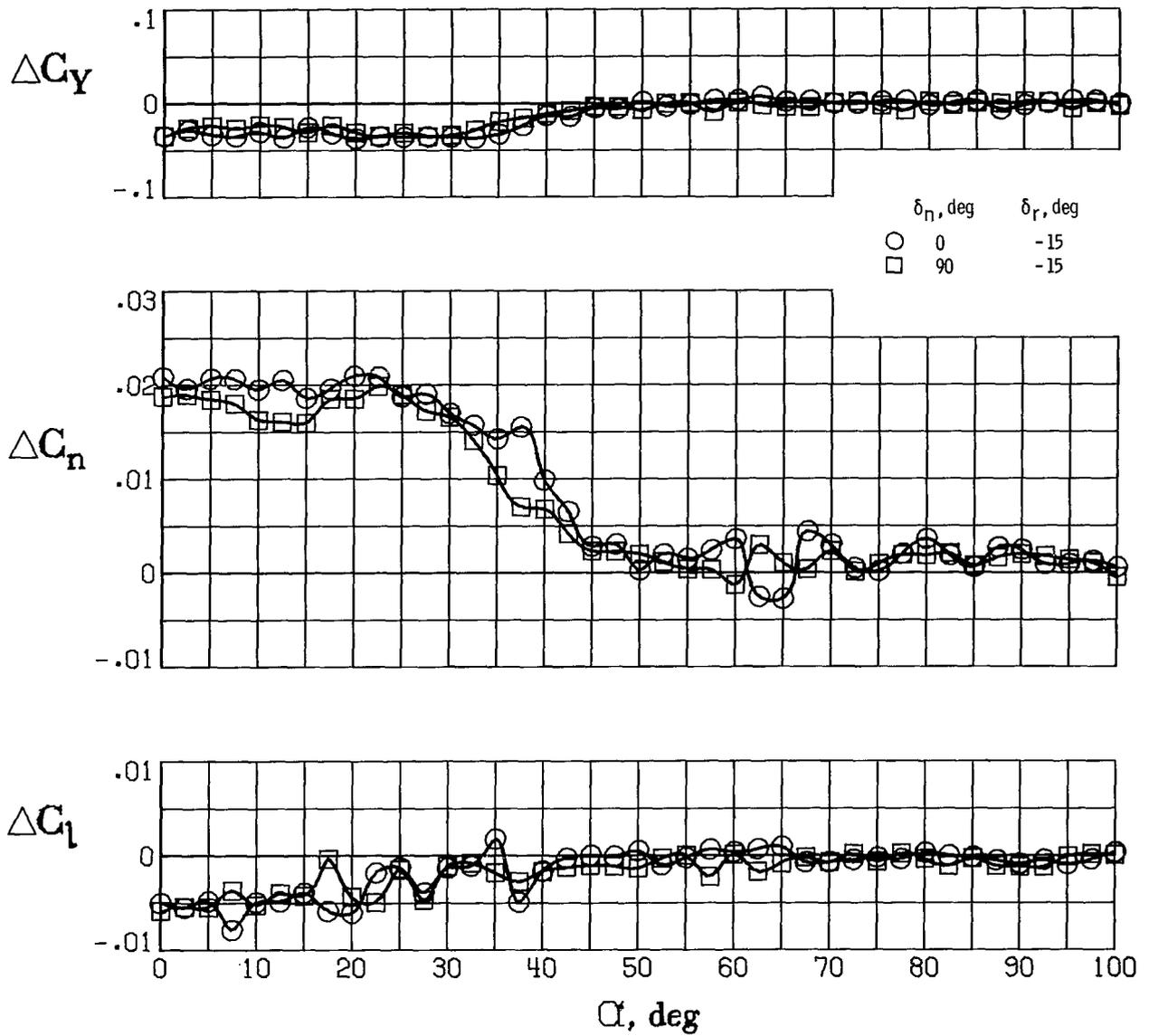
(a) Delta-wing configuration.

Figure 8.- Effect of rudder deflection.
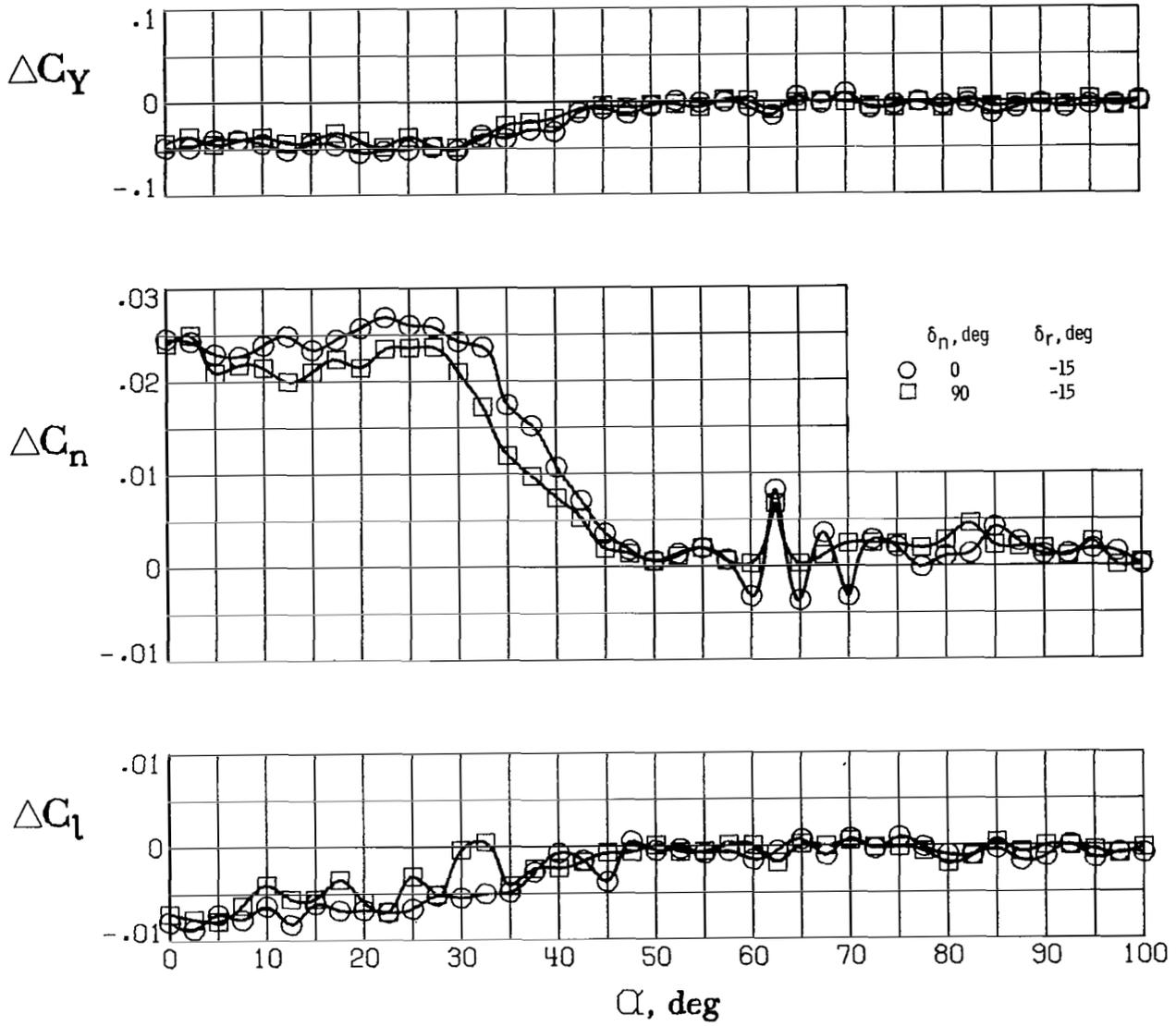
(b) Swept-wing configuration.

Figure 8.- Concluded.

(a) Delta-wing configuration.

Figure 9.- Effect of aileron deflection.
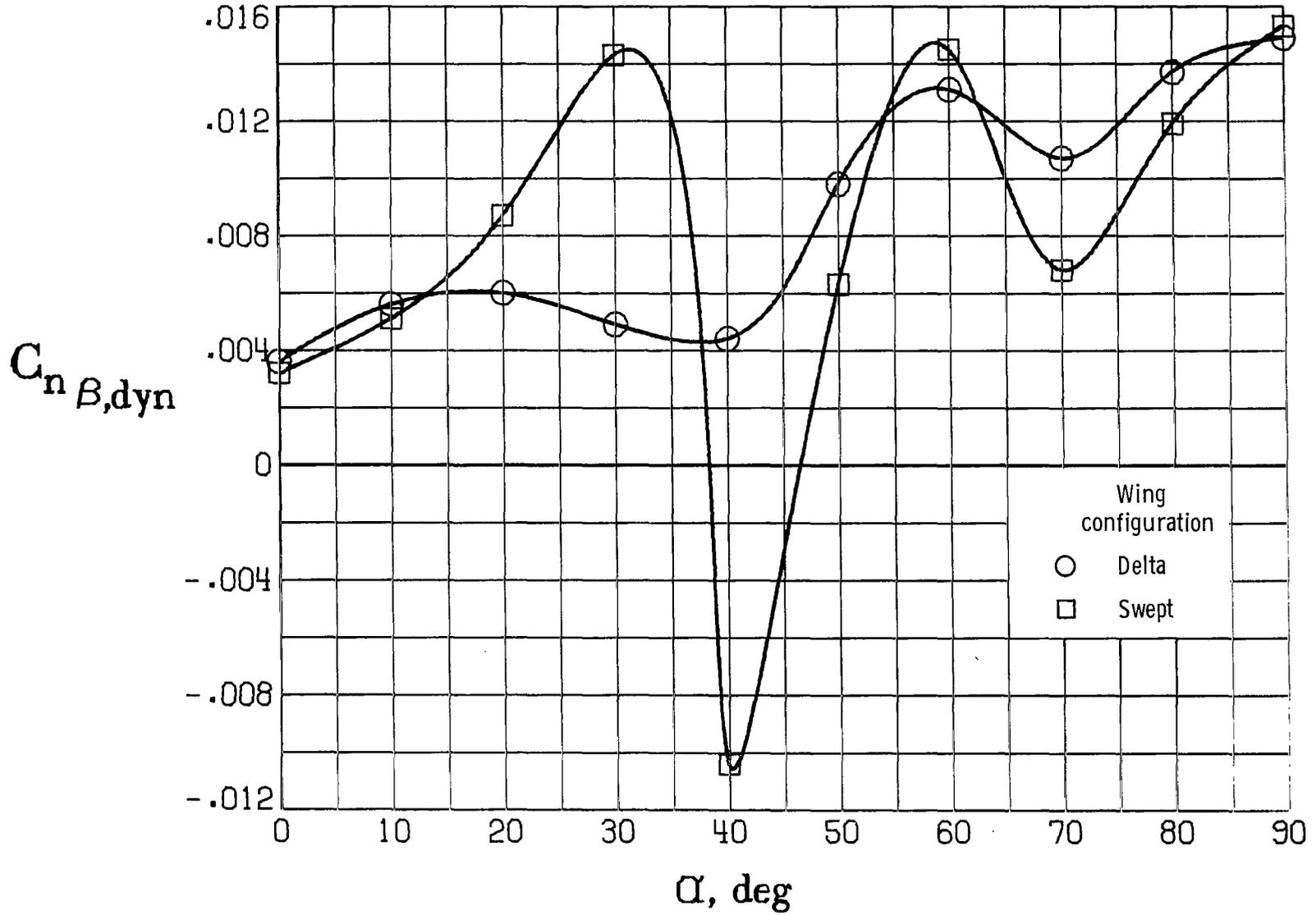
(b) Swept-wing configuration.

Figure 9.- Concluded.

Figure 10.- Variation of $C_{n_{\beta,dyn}}$ with angle of attack.

A motion-picture film supplement L-1186 is available on loan. Requests will be filled in the order received. You will be notified of the approximate date scheduled.

The film (16 mm, 8 min, color, silent) shows vertical take-offs, short hovering flights, and transition from hovering to normal forward flight for the delta- and swept-wing configurations.

Requests for the film should be addressed to:

NASA Langley Research Center
Att: Photographic Branch, Mail Stop 171
Hampton, Va. 23665

- - - - - - - - - - - - - - - - - CUT - - - - - - - - - - - - - - - - -

Date _____

Please send, on loan, copy of film supplement L-1186 to TN D-8054.

Name of organization _____

Street number _____

City and State _____ Zip code

Attention: Mr. _____

Title _____

"The aeronautical and space activities of the United States shall be conducted so as to contribute . . . to the expansion of human knowledge of phenomena in the atmosphere and space. The Administration shall provide for the widest practicable and appropriate dissemination of information concerning its activities and the results thereof."
—NATIONAL AERONAUTICS AND SPACE ACT OF 1958

NASA SCIENTIFIC AND TECHNICAL PUBLICATIONS

TECHNICAL REPORTS: Scientific and technical information considered important, complete, and a lasting contribution to existing knowledge.

TECHNICAL NOTES: Information less broad in scope but nevertheless of importance as a contribution to existing knowledge.

TECHNICAL MEMORANDUMS: Information receiving limited distribution because of preliminary data, security classification, or other reasons. Also includes conference proceedings with either limited or unlimited distribution.

CONTRACTOR REPORTS: Scientific and technical information generated under a NASA contract or grant and considered an important contribution to existing knowledge.

TECHNICAL TRANSLATIONS: Information published in a foreign language considered to merit NASA distribution in English.

SPECIAL PUBLICATIONS: Information derived from or of value to NASA activities. Publications include final reports of major projects, monographs, data compilations, handbooks, sourcebooks, and special bibliographies.

TECHNOLOGY UTILIZATION PUBLICATIONS: Information on technology used by NASA that may be of particular interest in commercial and other non-aerospace applications. Publications include Tech Briefs, Technology Utilization Reports and Technology Surveys.

Details on the availability of these publications may be obtained from:

SCIENTIFIC AND TECHNICAL INFORMATION OFFICE

NATIONAL AERONAUTICS AND SPACE ADMINISTRATION
Washington, D.C. 20546